



ACADEMIC
PRESS

Available online at www.sciencedirect.com

SCIENCE @ DIRECT®

Journal of Sound and Vibration 260 (2003) 403–416

JOURNAL OF
SOUND AND
VIBRATION

www.elsevier.com/locate/jsvi

Creep and shrinkage effect on the dynamic analysis of reinforced concrete slab-and-beam structures

E.J. Sapountzakis*, J.T. Katsikadelis

Department of Civil Engineering, Institute of Structural Analysis, National Technical University of Athens, Zografou Campus, GR - 157 73 Athens, Greece

Received 3 July 2001; accepted 15 April 2002

Abstract

In this paper, a solution to the dynamic problem of reinforced concrete slab-and-beam structures including creep and shrinkage effects is presented. The adopted model takes into account the resulting in-plane forces and deformations of the plate as well as the axial forces and deformations of the beam, due to the combined response of the system. The analysis consists of isolating the beams from the plate by sections parallel to the lower outer surface of the plate. The influence on creep and shrinkage effects of the time between the casting and the loading of the plate and the beams is taken into account. A lumped mass matrix is constructed from the tributary mass areas to the nodal mass points and a stiffness matrix is computed using the solution of the corresponding static problem. Both free and forced vibrations are considered and numerical examples of practical interest are presented. The discrepancy between the eigenvalues obtained using the present analysis, which better approximates to the actual response of the plate-beam system and the corresponding ones which ignore the in-plane forces and deformations requires the adopted model.

© 2002 Elsevier Science Ltd. All rights reserved.

1. Introduction

The interest in reinforced concrete slab-and-beam structures has been widespread in recent years due to the economic and structural advantages of such systems. Stiffened reinforced concrete plate structures are efficient, economical and functional, while construction using precast beams is the quickest, most usual and economical method for long river/or valley bridges or for long-span slabs. The extensive use of plate structures necessitates a rigorous static and dynamic analysis.

*Corresponding author. Tel.: +301-772-1718; fax: +301-772-1720.

E-mail address: cvsapoun@central.ntua.gr (E.J. Sapountzakis).

Although there is extensive literature on static analysis of these systems [1–10], to the authors' knowledge only a limited amount of technical literature is available on the dynamic analysis of stiffened plate systems, limited to evaluating bounds of eigenfrequencies using the Rayleigh–Ritz procedure [11,12] or employing the finite element method [13]. In previous work the adopted model for the dynamic analysis of plate–beams systems consists of isolating the beams from the plate and neglecting the shear forces at the interfaces. This assumption results in considerable discrepancies from the actual response of the stiffened plate. Moreover, it does not allow these forces to be determined, which are necessary for the design of composite or prefabricated structures.

In this paper the dynamic analysis of reinforced concrete slab-and-beam structures is presented. The adopted structural model is that employed by Sapountzakis and Katsikadelis [10], which, contrary to the models used previously, takes into account the resulting in-plane forces and deformations of the plate as well as the axial forces and deformations of the beam, due to combined response of the system. Using this model, the study of the dynamic behaviour of a stiffened plate subjected to a lateral load and to the effects of creep and shrinkage, either for simultaneous or for separate casting of the plate and the beams is attempted. The method presented employs the static solution to establish a flexibility matrix with respect to a set of nodal mass points in the interior of the plate. The mass matrix is constructed by lumping the mass areas contributing to the nodal mass points of the discretized plate [14, 15]. The static solution is obtained using the analogue equation method (AEM) [16]. The analysis consists in isolating the beams from the plate by sections parallel to the lower outer surface of the plate. The forces at the interface, which produce lateral deflection and in-plane deformation of the plate and lateral deflection and axial deformation of the beam, are established using continuity conditions at the interface. Both free and forced transverse vibrations are considered and numerical examples of practical interest are presented. The discrepancy between the eigenfrequencies obtained using the analysis presented, which better approximates to the actual response of the plate–beam system, and the corresponding ones which ignore the in-plane forces and deformations, justify the analysis used in the proposed model. Finally, the influence of the time interval between the casting of the plate and the beams on the dynamic behaviour of the stiffened plate is examined.

2. Statement of the problem

Consider a thin reinforced concrete plate having constant thickness h_p , occupying the domain Ω of the x, y plane and stiffened by a set of parallel reinforced concrete beams. The plate may have J holes and is supported on its boundary $\Gamma = \bigcup_{j=0}^J \Gamma_j$, which may be piecewise smooth (Fig. 1), while the beams may have point supports. For the sake of convenience the x -axis is taken parallel to the beams.

Let the time of the casting of the beams t_{bc} be the beginning of the time considered t , t_{bl} be the time at initial loading of the beams, t_{pc} be the time of the casting of the plate and t_{pl} be the time at which the plate is initially subjected to the lateral load $g = g(\mathbf{x}, t)$, $\mathbf{x} : \{x, y\}$, $t \geq 0$.

The solution of the problem at hand is approached by isolating the beams from the plate by sections in the lower outer surface of the plate and taking into account the tractions at the fictitious interfaces (Fig. 2). These tractions result in the loading of the beam as well as the

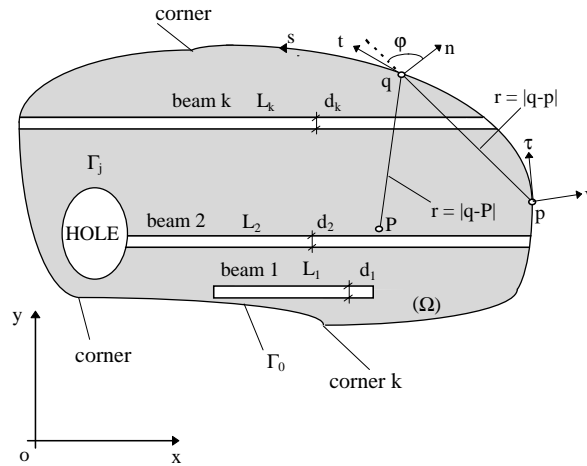


Fig. 1. Two-dimensional region Ω occupied by the plate.

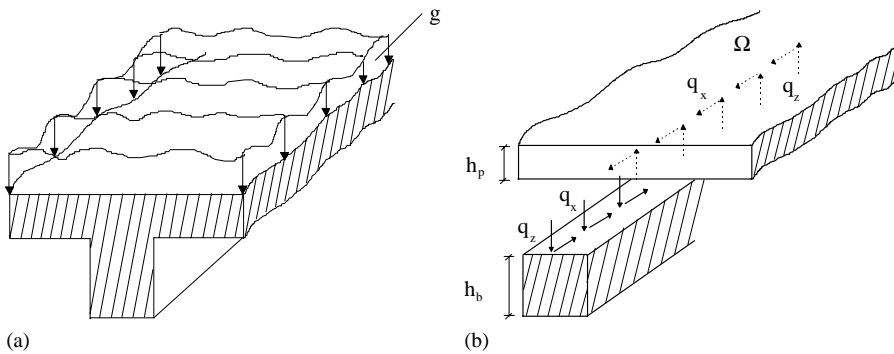


Fig. 2. Thin elastic plate stiffened by beams (a) and isolation of the beams from the plate (b).

additional loading of the plate. Their distribution is unknown and can be established by imposing displacement continuity conditions at the interfaces and using the procedure developed in this investigation.

The integration of the tractions along the width of the beam result in line forces per unit length which are denoted by q_x , q_y and q_z . Taking into account that the torsional stiffness of the beam is small, the traction component q_y , in the direction normal to the beam axis, may be ignored. However, in a more refined model the influence of this component may also be considered. The other two components q_x and q_z produce the following loadings along the trace of each beam:

(a) *In the plate*

- (i) A lateral line load $-q_z$ at the interface.
- (ii) A lateral line load $-\partial M_p / \partial x$ due to the eccentricity of the component q_x from the middle surface of the plate. $M_p = q_x h_p / 2$ is the bending moment.
- (iii) An in-plane line body force q_x at the middle surface of the plate.

(b) *In each beam*

- (i) A transverse load q_z .
- (ii) A transverse load $\partial M_b / \partial x$ due to the eccentricity of q_x from the neutral axis of the beam cross-section.
- (iii) An in-plane axial force q_x .

The structural models of the plate and the beams are shown in Fig. 3.

Following from the above considerations the response of the plate and of the beams may be described by the following initial boundary value problems.

2.1. *For the plate*

The plate undergoes transverse deflection and in-plane deformation. Thus, for the transverse deflection

$$\begin{aligned}
 & D \nabla^4 w_p + \rho_p \ddot{w}_p - \left(N_x \frac{\partial^2 w_p}{\partial x^2} + 2N_{xy} \frac{\partial^2 w_p}{\partial x \partial y} + N_y \frac{\partial^2 w_p}{\partial y^2} \right) \\
 & = g - \sum_{k=1}^K \left(q_z^{(k)} + \frac{\partial M_p^{(k)}}{\partial x} \right) \delta(y - y_k) \quad \text{in } \Omega,
 \end{aligned} \tag{1}$$

$$\alpha_1 w_p + \alpha_2 V_n = \alpha_3 \quad \text{on } \Gamma, \tag{2a}$$

$$\beta_1 \frac{\partial w_p}{\partial n} + \beta_2 M_n = \beta_3, \tag{2b}$$

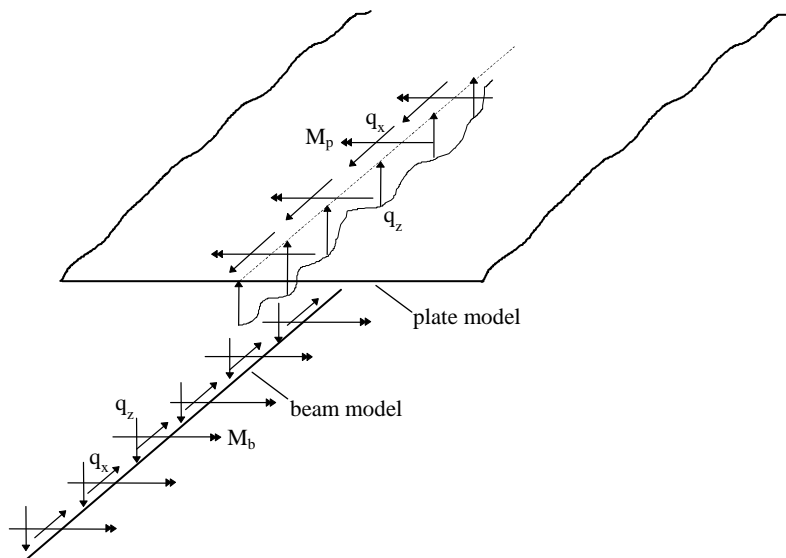


Fig. 3. Structural model of the plate and the beams.

$$w_p(\mathbf{x}, 0) = \varepsilon(\mathbf{x}), \tag{3a}$$

$$\dot{w}_p(\mathbf{x}, 0) = \bar{\varepsilon}(\mathbf{x}), \tag{3b}$$

where $w_p = w_p(\mathbf{x}, t)$, is the transverse deflection of the plate; $D(t) = E_p(t)h_p^3/12(1 - \nu^2)$ is its time-dependent flexural rigidity with E_p being the elastic modulus and ν the Poisson ratio; $N_x = N_x(\mathbf{x}, t)$, $N_y = N_y(\mathbf{x}, t)$, $N_{xy} = N_{xy}(\mathbf{x}, t)$ are the membrane forces per unit length of the plate cross-section at time t ; $\rho_p = \rho h_p$ is the surface mass density of the plate with ρ being the volume mass density; $\delta(y - y_k)$ is the Dirac's delta function in the y direction; $\varepsilon(\mathbf{x})$, $\bar{\varepsilon}(\mathbf{x})$ are the initial deflection and the initial velocity of the points of the middle surface of the plate; M_n and V_n are the bending moments normal to the boundary and the effective reaction along it, respectively, and they are given as

$$M_n = -D \left(\frac{\partial^2 w_p}{\partial n^2} + \nu \frac{\partial^2 w_p}{\partial t^2} \right), \tag{4}$$

$$V_n = -D \left[\frac{\partial}{\partial n} \nabla^2 w_p - (\nu - 1) \frac{\partial}{\partial s} \frac{\partial^2 w_p}{\partial n \partial t} \right]. \tag{5}$$

Finally, a_i, β_i ($i=1,2,3$) are functions specified on the boundary Γ . For the purposes of this investigation the material behaviour of the reinforced concrete plate is assumed to be linearly elastic (service state conditions).

The boundary conditions (2a) and (2b) are the most general linear boundary conditions for the plate problem including also the elastic support. It is apparent that all types of the conventional boundary conditions (clamped, simply supported, free or guided edge) can be derived from these equations by specifying the functions a_i and β_i appropriately (e.g., for a clamped edge it is $a_1 = \beta_1 = 1, a_2 = a_3 = \beta_2 = \beta_3 = 0$).

If the stresses are kept within the limits corresponding to the normal service conditions, assuming a linear relationship between creep and the stress causing the creep and denoting by $t_p = t_{pl} - t_{pc}$, Trost's theory [17] gives the tangent modulus of elasticity as

$$E_p(t) = \frac{E_{pl}}{1 + \chi \varphi(t, t_p)}, \tag{6}$$

where E_{pl} is the tangent modulus of elasticity of the plate at time t_p , χ is an ageing coefficient depending on strain development with time, $\varphi(t, t_p)$ is the creep coefficient related to the elastic deformation at t_p days which is defined as [18]

$$\varphi(t, t_p) = \phi_{RH} \beta(f_{cm}) \beta(t_p) \beta_{cp}(t - t_p), \tag{7}$$

where ϕ_{RH} , $\beta(f_{cm})$ and $\beta(t_p)$ are the factors depending on the relative humidity, the concrete strength and the concrete age at loading, respectively, which are defined as

$$\phi_{RH} = 1 + (1 - RH/100)/(0.10 \sqrt[3]{h_0}), \tag{8a}$$

$$\beta(f_{cm}) = 16.8/\sqrt{f_{cm}}, \tag{8b}$$

$$\beta(t_p) = 1/(0.1 + t_p^{0.20}), \tag{8c}$$

where RH is the relative humidity of the ambient environment in %, $h_0 = 2A_p/u_p$ is the notional size of the plate in mm, A_p is the area of the plate cross-section, u_p is the plate perimeter in contact with the atmosphere, f_{cm} is the mean compressive strength of concrete in N/mm^2 at the age of 28 days. Moreover, $\beta_{cp}(t - t_p)$ in Eq. (7) is a coefficient for the development of creep with time, which is estimated from

$$\beta_{cp}(t - t_p) = [(t - t_p)/(\beta_H + t - t_p)]^{0.3}, \quad (9)$$

where β_H is a coefficient depending on the relative humidity RH , given as

$$\beta_H = 1.5[1 + (0.012RH)^{18}]h_0 + 250 \leq 1500. \quad (10)$$

Since linear plate bending theory is considered, the components of the membrane forces N_x , N_y , N_{xy} do not depend on the deflection w_p . They are given as

$$N_x = C \left(\frac{\partial u_p}{\partial x} + \nu \frac{\partial v_p}{\partial y} \right), \quad (11a)$$

$$N_y = C \left(\nu \frac{\partial u_p}{\partial x} + \frac{\partial v_p}{\partial y} \right), \quad (11b)$$

$$N_{xy} = C \frac{1 - \nu}{2} \left(\frac{\partial u_p}{\partial y} + \frac{\partial v_p}{\partial x} \right), \quad (11c)$$

where $C(t) = E_p(t)/(1 - \nu^2)$; $u_p = u_p(\mathbf{x}, t)$ and $v_p = v_p(\mathbf{x}, t)$ are the displacement components of the middle surface of the plate arising from both the line body force q_x and the plate shrinkage, which is conveniently expressed in terms of a uniform variation of temperature $T_p(\mathbf{x}, t)$. The above displacement components are established by solving independently the plane stress problem, which is described by the following quasi-static (in-plane inertia forces are ignored) boundary value problem (Navier's equations of equilibrium):

$$\nabla^2 u_p + \frac{1 + \nu}{1 - \nu} \frac{\partial}{\partial x} \left[\frac{\partial u_p}{\partial x} + \frac{\partial v_p}{\partial y} \right] + \frac{1}{G_p} q_x \delta(y - y_k) - 2\alpha \frac{(1 + \nu)}{(1 - \nu)} \frac{\partial T_p}{\partial x} = 0, \quad \text{in } \Omega \quad (12a)$$

$$\nabla^2 v_p + \frac{1 + \nu}{1 - \nu} \frac{\partial}{\partial y} \left[\frac{\partial u_p}{\partial x} + \frac{\partial v_p}{\partial y} \right] - 2\alpha \frac{1 + \nu}{1 - \nu} \frac{\partial T_p}{\partial y} = 0, \quad (12b)$$

$$\gamma_1 u_n + \gamma_2 N_n = \gamma_3 \quad \text{on } \Gamma, \quad (13a)$$

$$\delta_1 u_t + \delta_2 N_t = \delta_3 \quad (13b)$$

in which $G_p(t) = E_p(t)/2(1 + \nu)$ is the shear modulus of the plate; α is the linear coefficient of thermal expansion; N_n , N_t and u_n , u_t are the boundary membrane forces and displacements in the normal and tangential directions to the boundary, respectively; γ_i , δ_i ($i = 1, 2, 3$) are functions specified on Γ .

Assuming that creep and shrinkage are independent, the temperature distribution $T_p(\mathbf{x}, t)$ is given as [18]

$$T_p(\mathbf{x}, t) = \varepsilon_{sp}(t - t_{pc})/\alpha, \quad (14)$$

where $\varepsilon_{sp}(t - t_{pc})$ is the shrinkage strain calculated from

$$\varepsilon_{sp}(t - t_{pc}) = \varepsilon_{sp}(f_{cm})\beta_{RH}\beta_{sp}(t - t_{pc}), \tag{15}$$

where $\varepsilon_{sp}(f_{cm})$, β_{RH} are the factors depending on the concrete strength and the relative humidity, respectively, which are defined as

$$\varepsilon_{sp}(f_{cm}) = [160 + \beta_{sc}(90 - f_{cm})]10^{-6}, \tag{16a}$$

$$\beta_{RH} = \begin{cases} -1.55(1 - (RH/100)^3) & \text{for } 40\% \leq RH \leq 99\% \text{ (stored in air)} \\ +0.25(1 - (RH/100)^3) & \text{for } RH \geq 99\% \text{ (immersed in water),} \end{cases} \tag{16b}$$

where β_{sc} is a coefficient depending on type of cement. Moreover, $\beta_{sp}(t - t_{pc})$ in Eq. (15) is a coefficient for the development of shrinkage with time, which is estimated from

$$\beta_{sp}(t - t_{pc}) = [(t - t_{pc})/(0.035h_0^2 + t - t_{pc})]^{0.5}. \tag{17}$$

2.2. For each beam

Each beam undergoes transverse deflection and axial deformation. Thus, for the transverse deflection, assuming (as for the plate for the reinforced concrete beam) linearly elastic material behaviour (service state conditions):

$$E_b I_b \frac{d^4 w_b}{dx^4} + \rho_b \ddot{w}_b - N_b \frac{\partial^2 w_b}{\partial x^2} = q_z - \frac{\partial M_b}{\partial x} \quad \text{in } L_k, k = 1, 2, \dots, K, \tag{18}$$

$$a_1 w_b + a_2 V = a_3, \tag{19a}$$

$$b_1 \frac{\partial w_b}{\partial x} + b_2 M = b_3 \quad \text{at the beam ends } x = 0, l, \tag{19b}$$

$$w_b(x, 0) = e(x), \tag{20a}$$

$$\dot{w}_b(x, 0) = \bar{e}(x), \tag{20b}$$

where $w_b = w_b(x, t)$ is the transverse deflection of the beam; I_b is its moment of inertia; $N_b = N_b(x, t)$ is the axial force at the neutral axis; V, M are the reaction and the bending moment at the beam ends, respectively; ρ_b is the surface mass density of the beam; $a_i, b_i (i = 1, 2, 3)$ are the coefficients specified at the boundary of the beam; $e(x), \bar{e}(x)$ are the initial deflection and the initial velocity of the points of the neutral axis of the beam. It is worth noting that the initial deflection and velocity of the points of the middle surface of the plate $\varepsilon(\mathbf{x}), \bar{\varepsilon}(\mathbf{x})$ must comply with the initial deflection and velocity of the points of the neutral axis of the beam $e(x), \bar{e}(x)$ since the plate and the beams are assumed to be firmly bonded together.

Finally, $E_b = E_b(t)$ is the time-dependent tangent modulus of elasticity of the beam given as [17]

$$E_b(t) = \frac{E_{bt}}{1 + \chi\varphi(t, t_b)}, \tag{21}$$

where E_{bt} is the tangent modulus of elasticity of the beam at time t_{bt} , χ is an ageing coefficient depending on strain development with time, $t_b = t_{bt} - t_{bc}$; $\varphi(t, t_b)$ is the creep coefficient related to

the elastic deformation at t_b days, which is defined [18] as

$$\varphi(t, t_b) = \phi_{RH}\beta(f_{cm})\beta(t_b)\beta_{cb}(t - t_b), \tag{22}$$

where ϕ_{RH} , $\beta(f_{cm})$, $\beta(t_b)$ and $\beta_{cb}(t - t_b)$ are two creep coefficients for the beam similar to those for the plate.

It is apparent that all types of the conventional boundary conditions (clamped, simply supported, free or guided edge) can be derived from Eqs. (19a) and (19b) by specifying the coefficients a_i , b_i appropriately (e.g., for a simply supported end it is $a_1 = b_2 = 1$, $a_2 = a_3 = b_1 = b_3 = 0$).

Since linear beam bending theory is considered, the axial force of the beam does not depend on the deflection w_b . The axial deformation of the beam arising from both the in-plane axial force q_x and the beam shrinkage, which is conveniently expressed in terms of a uniform variation of temperature $T_b(x, t)$, is described by solving independently the following quasi-static (axial inertia forces are neglected) boundary value problem, i.e.,

$$E_b A_b \frac{\partial^2 u_b}{\partial x^2} = -q_x + \alpha \frac{\partial T_b}{\partial x} \quad \text{in } L_k, k = 1, 2, \dots, K, \tag{23}$$

$$c_1 u_b + c_2 N = c_3 \quad \text{at the beam ends } x = 0, l, \tag{24}$$

where N is the axial reaction at the beam ends.

Similarly to the plate, the temperature distribution T_b for the beam is given as

$$T_b = \varepsilon_{sb}(t - t_{bc})/\alpha, \tag{25}$$

where

$$\varepsilon_{sb}(t - t_{bc}) = \varepsilon_{sb}(f_{cm})\beta_{RH}\beta_{sb}(t - t_{bc}), \tag{26}$$

where $\varepsilon_{sp}(f_{cm})$, β_{RH} , $\beta_{sb}(t - t_{bc})$ are the shrinkage coefficients for the beam similar to those for the plate.

Eqs. (1), (12a), (12b), (18), (23) constitute a set of five coupled partial differential equations including seven unknowns, namely $w_p, u_p, v_p, w_b, u_b, q_x, q_z$. Two additional equations are required, which result from the continuity conditions of the displacements in the direction of the z and x axes at the interfaces between the plate and the beams. These conditions can be expressed as

$$w_p = w_b, \tag{27}$$

$$u_p - \frac{h_p}{2} \frac{\partial w_p}{\partial x} = u_b + \frac{h_b}{2} \frac{\partial w_b}{\partial x}. \tag{28}$$

It must be noted that the coupling of Eqs. (1), (12a) and (2b), as well as of Eqs. (18) and (23) is non-linear due to the terms including the unknown membrane and axial forces, respectively.

3. Solution procedure

The solution of the dynamic problem requires the integration of the set of Eqs. (1), (12a), (12b), (18) and (23) subjected to the prescribed boundary and initial conditions. An analytic solution of this problem is out of the question. Therefore, recourse to a numerical solution is inevitable. The

method presented by Katsikadelis and Kandilas [14] is employed in this investigation. According to this method, the domain Ω occupied by the plate is discretized by establishing a system of M nodal points on it, corresponding to M mass cells, to which masses are assigned according to the lumped mass assumption. Care is taken so that nodal points are placed on the traces of the beams (Fig. 4). Subsequently, the stiffness matrix as well as the load vector with respect to the nodal points is established. This procedure leads to the typical equation of motion for the stiffened plate

$$[\mathbf{m}]\{\ddot{\mathbf{w}}\} + [\mathbf{k}]\{\mathbf{w}\} = \{\mathbf{g}\}, \tag{29}$$

where $\{\mathbf{w}\}$ is a vector including the deflections at the M domain nodal points, $[\mathbf{m}]$ is the mass matrix, $[\mathbf{k}]$ is the stiffness matrix and $\{\mathbf{g}\}$ is the nodal load vector.

The mass matrix $[\mathbf{m}]$ is diagonal. Its elements m_i are readily computed by lumping the mass area contributing to the i nodal point. The elements g_i of the load vector $\{\mathbf{g}\}$ are computed from the mean value of $g(\mathbf{x})$ on each element.

The stiffness matrix $[\mathbf{k}]$ with respect to the M domain nodal points is obtained by inverting the flexibility matrix $[\mathbf{f}]$. The latter is established by solving the static problem by working as follows. The typical element f_{ij} is computed as the static deflection at point i due to a unit load at point j . It is apparent that $M(M - 1)$ static solutions are required since the flexibility matrix is symmetric. The static problem results from the same equations (Eqs. (1), (12a), (12b), (18), (23)) under the prescribed boundary conditions by neglecting the inertia forces. The solution is achieved using the AEM as presented in detail by Sapountzakis and Katsikadelis [10, 16].

(a) *Forced vibrations.* For forced vibrations it is $[k] = [f]^{-1}$, and Eq. (29) can be solved using any time step integration scheme. The initial conditions in this case are

$$\{\mathbf{w}(0)\} = \{\boldsymbol{\varepsilon}\}, \quad \{\dot{\mathbf{w}}(0)\} = \{\boldsymbol{\xi}\} \tag{30}$$

(b) *Free vibrations.* For free vibrations, $\{\mathbf{g}\} = \{\mathbf{0}\}$. By setting

$$\{\mathbf{w}(t)\} = \{\mathbf{W}\} e^{-i\omega t}, \tag{31}$$

the following typical eigenvalue problem is obtained:

$$\left([\mathbf{f}][\mathbf{m}] - \frac{1}{\omega_i^2} [\mathbf{I}] \right) \{\mathbf{W}\} = 0, \tag{32}$$

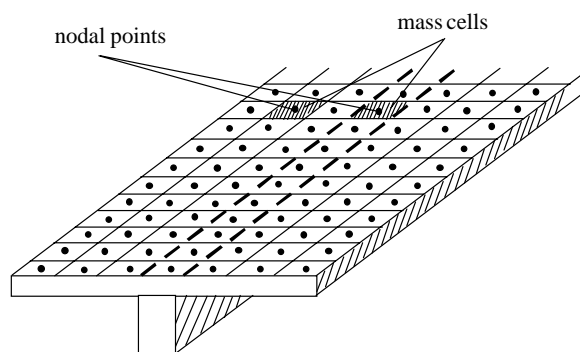


Fig. 4. Discretization of the plate.

where $[I]$ is the unit matrix, from which the M eigenfrequencies and mode shapes can be established.

4. Numerical examples

On the basis of the analytical and numerical procedures presented in the previous Sections, a computer program has been written and representative examples have been studied to demonstrate the efficiency and the range of applications of the developed method. In all the examples treated, the numerical results have been obtained using 54 constant boundary elements and 162 constant domain rectangular cells. The following data have been used for the numerical results: concrete C25/30, $f_{cm} = 25 \text{ N/mm}^2$, $RH=40\%$, $t_p = t_b = 28$ days, $E_{pl} = E_{bl} = E_{c28} = 32.55 \text{ kN/mm}^2$, $h_p = 0.20 \text{ m}$, $\nu = 0.154$, $\beta_{sc} = 5$ (normal or rapid hardening cement), $\alpha = 10^{-5} \text{ } ^\circ\text{C}$.

4.1. Example 1

(a) *Free vibrations.* The free vibrations of a rectangular plate with side lengths $a_p = 18.0 \text{ m}$ and $b_p = 9.0 \text{ m}$, stiffened by a beam of rectangular cross-section $1.0 \text{ m} \times h_b$ placed along its x -axis of symmetry (Fig. 5) have been studied. The edges of the plate along the x -axis are free, while the other two are simply supported according to the transverse boundary conditions. Moreover, $u_x = u_y = 0$ at $x = 0, a_p$ while $N_x = N_{xy} = 0$ at $y = \pm b_p/2$ according to the in-plane boundary conditions. In this example, both the plate and the beam are simultaneously casted ($t_{bc} = t_{pc} = 0$). In Table 1 the first 10 computed eigenfrequencies along with the corresponding mode shapes and their contours of the plate – beam system with $h_b = 0.60 \text{ m}$ for various instants are presented. Moreover, in Table 2 the fundamental eigenfrequency for various values of the beam height h_b and for various instants are presented as compared with those obtained from the developed model ignoring the in-plane forces and deformations of the plate as well as the axial forces and deformations of the beam.

From both tables it is worth noting that the eigenfrequencies obtained decrease with time due to the predominant action of creep compared to shrinkage. As expected, the influence of creep action is more significant in the early ageing of concrete. Moreover, the discrepancy from the results obtained from the numerical solution ignoring the in-plane forces and deformations is remarkable.

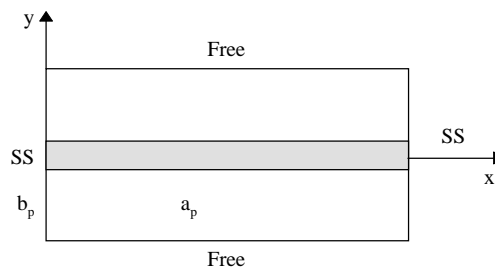


Fig. 5. Plan of the stiffened plate.

Table 1
Eigenfrequencies $\Omega = \omega\sqrt{\rho}$ of the plate of Example 1 for various instants t (days)

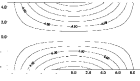
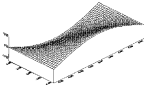
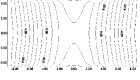
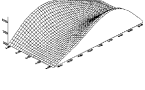

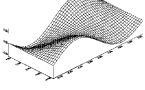
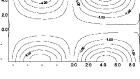
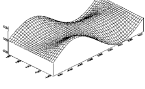
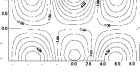
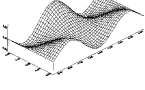
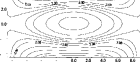
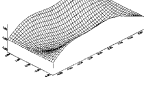

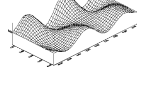

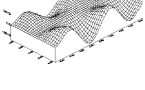
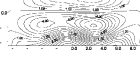
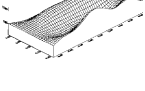
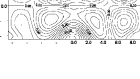
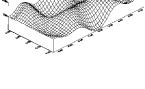
Ω_m	Contours	Mode shapes	$t = 30$	$t = 100$	$t = 300$	$t = 1000$
Ω_1			8.309	6.719	6.359	6.285
Ω_2			15.131	12.032	11.004	10.490
Ω_3			19.300	15.478	14.503	14.169
Ω_4			25.554	20.286	18.667	17.947
Ω_5			34.931	27.717	26.363	23.497
Ω_6			35.793	28.467	26.390	25.454
Ω_7			41.537	32.894	30.039	28.961
Ω_8			59.938	47.379	43.589	41.645
Ω_9			65.117	51.385	47.095	44.902
Ω_{10}			71.953	56.211	50.889	47.576

Table 2

Fundamental eigenfrequencies of the stiffened plate of Example 1 for various values of the beam height h_b and for various instants t (model I) compared with those obtained ignoring the in-plane forces and deformations (model II)

Age of concrete t (days)	Stiffening beam					
	1.00 × 0.20		1.00 × 0.60		1.00 × 2.00	
	Model I	Model II	Model I	Model II	Model I	Model II
30	7.6265	3.4256	15.1310	7.9812	17.8186	9.5305
100	6.2080	2.6924	12.0319	6.2397	14.0262	7.5698
300	5.9497	2.4481	11.0039	5.6419	12.8172	6.8537
1000	5.9437	2.2836	10.4900	5.2678	11.4840	6.3659

Table 2

Table 3

Deflections w (m) at the centre and at the middle of the free side of the plate of Example 1 for various instants t

Age of concrete t (days)	Centre			Middle of the free side		
	Dynamic w_{max}	Static w_{st}	$D = \max R(t) $	Dynamic w_{max}	Static w_{st}	$D = \max R(t) $
30	0.0200	0.0091	2.19	0.0740	0.0332	2.22
100	0.0302	0.0133	2.27	0.1175	0.0491	2.39
300	0.0343	0.0148	2.32	0.1381	0.0531	2.60
1000	0.0410	0.0153	2.68	0.1530	0.0536	2.85

Table 3

(b) *Forced vibrations.* The forced vibrations of the examined stiffened plate have been studied when subjected to a suddenly applied uniformly distributed load q of infinite duration. In Table 3 the maximum values, w_{max} , of the deflection at the centre and at the middle of the free side of the plate for various instants t are shown together with the corresponding static ones, w_{st} , for the calculation of the dynamic magnification factor $D = \max|R(t)|$, $R(t) = w(t)/w_{st}$.

4.2. Example 2

The casting of the beam of the stiffened plate of Example 1 preceded the casting of the plate at a time interval of $T = t_{pc} - t_{bc}$ days. In Table 4 the time development of the fundamental eigenfrequency of the stiffened plate for the height of the stiffening beam $h_b = 0.60$ m and for different values of the time interval T is presented. From the results obtained it is concluded that the dynamic response of the reinforced concrete stiffened plate is not influenced from the time interval between the casting of the plate and the beams.

5. Concluding remarks

The dynamic analysis of reinforced concrete slab-and-beam structures including creep and shrinkage effects has been studied. A realistic model has been adopted, which, contrary to other approaches, takes into account the in-plane forces and deformations of the plate as well as the

Table 4

Fundamental eigenfrequency of the plate of Example 2 for various instants t and for various values of the time interval T

Age of concrete t (days)	Time interval T			
	30	100	300	1000
30	8.3093	8.3094	8.3095	8.3096
100	6.7187	6.7188	6.7189	6.7189
300	6.3593	6.3593	6.3594	6.3594
1000	6.2847	6.2847	6.2847	6.2847

Table 4

Fundamental eigenfrequency of the plate of Example 2 for various instants t and for various values of the time interval axial forces and deformations of the beams. The main conclusions that can be drawn from this investigation are:

- (a) The proposed model permits the study of the dynamic behaviour of a stiffened plate including the opposed effects of creep and shrinkage either for simultaneous or for separate casting of the plate and the beams.
- (b) The evaluated eigenfrequencies are decreased with time due to the predominant action of creep compared to shrinkage.
- (c) The influence of creep action is more significant in the early ageing of concrete.
- (d) The evaluated eigenfrequencies of the plate – beams system are found to exhibit considerable discrepancy from those of other models, which neglect in-plane and axial forces and deformations.
- (e) The adopted model permits the evaluation of the in-plane shear forces at the interface between the plate and the beams, the knowledge of which is important in the design of prefabricated plate beams structures (estimation of shear connectors).
- (f) Dynamic response of reinforced concrete slab-and-beam structures is not influenced by the time interval between the casting of the plate and the beams.

References

- [1] A.H. Sheikh, M. Mukhopadhyay, Analysis of stiffened plate with arbitrary planform by the general spline finite strip method, *Computers and Structures* 42 (1) (1992) 53–67.
- [2] A.R. Kukreti, E. Cheraghi, Analysis procedure for stiffened plate systems using an energy approach, *Computers and Structures* 46 (1993) 649–657.
- [3] Z.A. Siddiqi, A.R. Kukreti, Analysis of eccentrically stiffened plates with mixed boundary conditions using differential quadrature method, *Journal of Applied Mathematical Modeling* 22 (4) (1998) 251–275.
- [4] I.E. Harik, M. Guo, Finite element analysis of eccentrically stiffened plates in free vibration, *Computers and Structures* 49 (6) (1993) 1007–1015.
- [5] M. Tanaka, A.N. Bercin, A Boundary element method applied to the elastic bending problem of stiffened plates, *Boundary Element Method XIX* (1997) 203–212.
- [6] C. Hu, G.A. Hartley, Elastic analysis of thin plates with beam supports, *Engineering Analysis with Boundary Elements* 13 (1994) 229–238.

- [7] J.B. De Paiva, Boundary element formulation of building slabs, *Engineering Analysis with Boundary Elements* 17 (1996) 105–110.
- [8] S.F. Ng, M.S. Cheung, T. Xu, A combined boundary element and finite element solution of slab and slab-on-girder bridges, *Computers and Structures* 37 (1990) 1069–1075.
- [9] M.S. Cheung, G. Akhras, W. Li, Combined boundary element/finite strip analysis of bridges, *Journal of Structural Engineering* 120 (1994) 716–727.
- [10] E.J. Sapountzakis, J.T. Katsikadelis, Elastic deformation of ribbed plates under static, transverse and inplane loading, *Computers and Structures* 74 (2000) 571–581.
- [11] S. Peng-Cheng, H. Dade, W. Zongmu, Static, vibration and stability analysis of stiffened plates using B spline functions, *Computers and Structures* 27 (1) (1993) 73–78.
- [12] D.W. Fox, V.G. Sigillito, Bounds for eigenfrequencies of a plate with an elastically attached reinforcing rib, *International Journal of Solids Structures* 18 (3) (1982) 235–247.
- [13] A.G. Cubus, *Cedrus-3 User's References Manual*, Version 1.56. Software, Zürich, Switzerland, 1995.
- [14] J.T. Katsikadelis, C.B. Kandilas, A flexibility matrix solution of the vibration problem of plates based on the boundary element method, *Acta Mechanica* 83 (1990) 51–60.
- [15] J.T. Katsikadelis, F.T. Kokkinos, Static and dynamic analysis of composite shear walls by the boundary element method, *Acta Mechanica* 68 (1987) 231–250.
- [16] E.J. Sapountzakis, J.T. Katsikadelis, Creep and shrinkage effect on reinforced concrete slab-and-beam structures, *Proceedings of the International Congress "Creating with Concrete"*, Dundee, Scotland, September 6–10. 1999.
- [17] H. Trost, J. Wolff, Zur wirklichkeitsnahen Ermittlung der Beanspruchungen in abschnittsweise hergestellten Spannbetontragwerken, *Der Bauingenieur* 45 (1970) 155–169.
- [18] Eurocode No. 2. Design of concrete structures, Part 1: general rules and rules for buildings, Eurocode 2 Editorial Group, Brussel, 1991.